

Supporting Information

Fine Structural Features of Core-Shell Nanoscale Zero-Valent Iron(nZVI) Characterized with Aberration-Corrected Scanning Transmission Electron Microscopy (Cs-STEM)

Airong Liu, and Weixian Zhang¹

State Key Laboratory for Pollution Control and Resource Reuse,
School of Environmental Science and Engineering, Tongji University,
Shanghai 200092, China

Summary of SI. The SI contains detailed descriptions of experimental procedures. Figure S1 shows the schematic of HD-2700 STEM. Figure S2 shows infrared spectroscopy of fresh nZVI. Figure S3 shows x-ray diffraction (XRD) of fresh nZVI.

Scanning Transmission Electron Microscopy (STEM)

The instrument, Hitachi HD2700, is equipped with a cold-field-emission electron source, a CEOS hexapole aberration-corrector and a high-resolution electron energy-loss spectrometer. Below the sample stage, there are five detectors designed for nano-diffraction and for simultaneous acquisition of transmission imaging including ADF imaging and EELS (and spectroscopy

¹ To whom correspondence should be addressed. Tel: +86-21-6598-2684; Fax: +86-21-6598-5885
E-mail address: zhangwx@tongji.edu.cn (Wei-xian Zhang)

imaging). The CEOS probe corrector, located between the condenser lens and the objective lens, has two hexapoles and five electromagnetic round lenses, seven dipoles for alignment and one quadrupole and one hexapole for astigmatism correction. In a spherical-aberration-corrected electron microscope, the probe size d (measured in FWHM) as a function of the beam convergence half-angle is an incoherent sum of contributions from the source size, diffraction limit and chromatic aberration and is given by

$$d = \sqrt{4i_p / \beta\pi^2\alpha_1^2)^2 + (0.6\lambda / \alpha)^2 + (C_c\alpha(\Delta E / E))^2}$$
, where i_p is the probe current, β is the source brightness, λ is the electron wavelength at beam energy E , ΔE is the energy spread and C_c is the chromatic aberration constant of the probe-forming lens. The calculated minimum probe size for the instrument is 0.075nm ($C_c=1.5$ mm), whereas the experimentally obtained value using single uranium atoms is 0.08 nm.¹ A schematic of HD-2700 STEM is shown in Fig. S1.

STEM

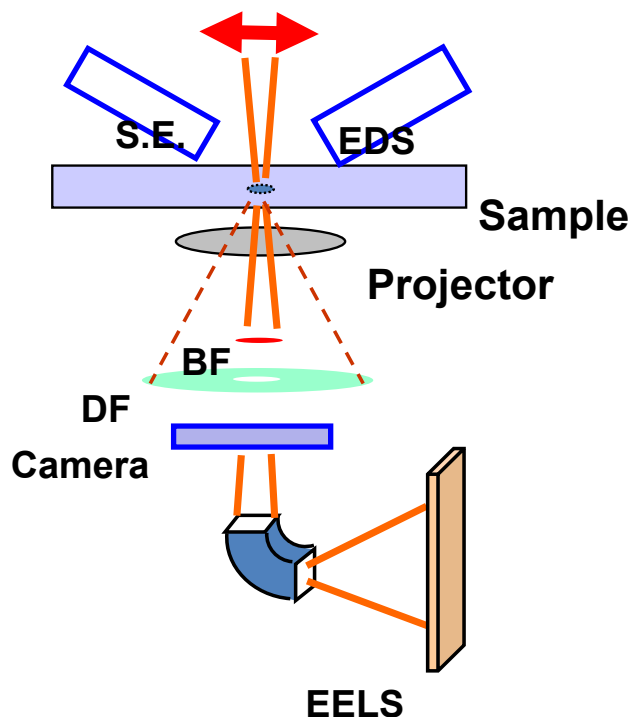


Fig. S1 A schematic of a HD-2700 STEM, showing the position of bright-field (BF) and high-angle annular dark-field (HAADF) detectors. As the probe is scanned across the specimen, the high collection angle of the HAADF detector records a signal dominated by incoherent, thermal diffuse scattering. This intensity is insensitive to sample thickness, probe defocus, and the coherent Bragg (diffraction) contrast characteristic of conventional transmission electron microscopy

Infrared Spectrum Analysis

Figure S2 represented the FTIR spectrum between 4000 to 400 cm^{-1} of fresh nZVI. It was reported that the band observed at 470 cm^{-1} can be attributed to the presence of hematite ($\alpha\text{-Fe}_2\text{O}_3$).² The peaks at 3448 and 1637 cm^{-1} were assigned to the O–H stretching vibration of H_2O , partly were due

to the O–H stretching vibration of FeOOH. From previous investigations by Cambier, the band at 670 cm^{-1} is due to the symmetric Fe-O stretch, and the broad band near 3120 cm^{-1} is attributable to the stretching mode of the bulk hydroxyl groups in the goethite(α -FeOOH) structure (ν_{OH}).³ The bands at 880 and 805 cm^{-1} can be assigned to the bending modes of bulk hydroxyl groups in the goethite structure. In fact, magnetite (Fe_3O_4) and maghemite (γ - Fe_2O_3) exhibit bands at 570 cm^{-1} and 630 cm^{-1} , respectively, which can be assigned to the Fe–O stretching modes of the tetrahedral and octahedral sites in their inverse spinel structure.⁴ The peaks at 1067 indicate the presence of γ -FeOOH-lepidocrocite.⁵ So we further conclude the surface of fresh nZVI is covered by the mixture of different iron oxide.

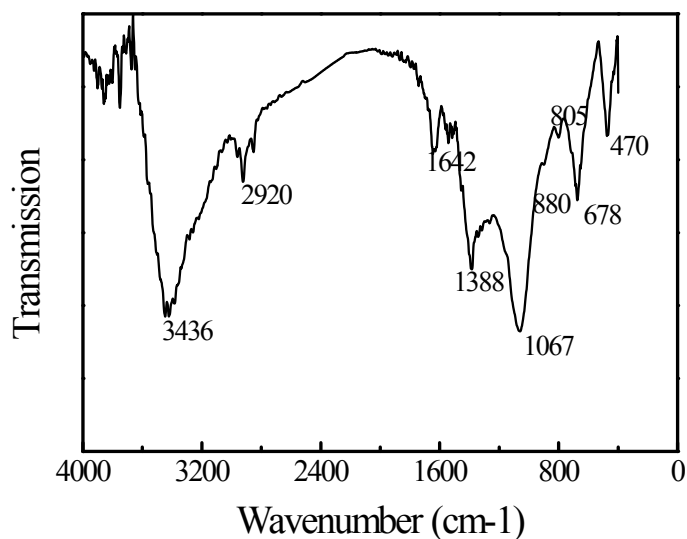


Fig. S2 FTIR spectra of the nZVI

X-ray Diffraction Analysis

The method of X-ray diffraction (XRD) was used to investigate the material structure of iron nanoparticles. The broad peak reveals the existence of an amorphous phase of iron. Apparent peak at the 2θ of 44.9° indicates the presence of zero-valent iron (α -Fe) crystalline phases, which is in good agreement with the High resolution STEM and corresponding SAED analysis of metallic core. Broad peaks at 35.8° and 31.8° indicate the presence of iron oxide (FeO) phases, but the iron oxide phase in the oxide layer seems not to be perfect crystalline, which is in agreement with the SAED results of STEM.⁶

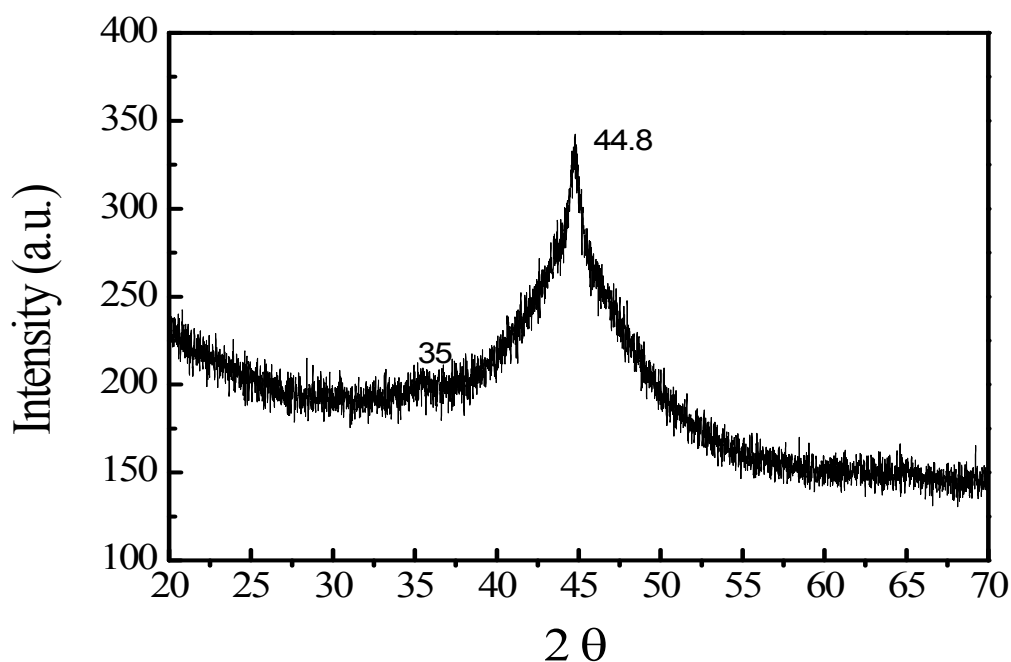


Fig. S3 XRD pattern of the nZVI.

Reference

1. Y. Zhu, H. Inada, K. Nakamura, J. Wall, Imaging single atoms using

secondary electrons with an aberration-corrected electron microscope, *Nature Mater.*, 2009, 8, 808-812.

2. Y.-S. Li, J. Church and A. Woodhead, Infrared and Raman spectroscopic studies on iron oxide magnetic nano-particles and their surface modifications, *J Magn. Magn. Mater.*, 2012, **324**, 1543–1550.
3. D. M. Cwiertny, G. J. Hunter, J. M. Pettibone, M. M. Scherer and V.H. Grassian, Surface Chemistry and Dissolution of γ -FeOOH Nanorods and Microrods: Environmental Implications of Size-Dependent Interactions with Oxalate, *J. Phys. Chem. C*, 2009, **113**, 2175–2186.
4. M. Baikousi, A. B. Bourlinos, A. Douvalis, T. Bakas, D. F. Anagnostopoulos, J. Tuček, K. Šafářová, R. Zboril and M. A. Karakassides, Synthesis and Characterization of γ -Fe₂O₃/Carbon Hybrids and Their Application in Removal of Hexavalent Chromium Ions from Aqueous Solutions, *Langmuir*, 2012, **28**, 3918–3930.
5. S. Bashkova and T. J. Bandosz, Adsorption/Reduction of NO₂ on Graphite Oxide/Iron Composites, *Ind. Eng. Chem. Res.*, 2009, **48**, 10884–10891.
6. Y. P. Sun, X. Q. Li, J. S. Cao, W.-X. Zhang and H.P. Wang, Characterization of zero-valent iron nanoparticles, *Adv. Colloid Interfac.*, 2006, **120**, 47–56.